Hyper-Chaotic and Chaotic Synchronisation of Two Interacting Dipoles

D. Urzagasti, D. Becerra-Alonso, L.M. Pérez, H.L. Mancini and D. Laroze

Abstract In the present work we study numerically the deterministic spin dynamics of two interacting anisotropic magnetic particles in the presence of a time dependent external magnetic field. The particles are coupled through their dipole-dipole interaction. The applied magnetic field is composed of a constant amplitude longitudinal component and other transversal with time dependent amplitude. The system is modelled by the dissipative Landau-Lifshitz equation. The different types of synchronisation have been studied finding that the system presents chaotic anti-synchronisation of the canonical component, for a wide range of parameters. Finally, we also found that the system exhibits phase hyper-chaotic synchronisation.

1 Introduction

Theoretical studies on the dynamics of magnetisation reversal are normally based either on the Landau-Lifshitz [1] equation or on the Landau-Lifshitz-Gilbert equation [2]. These models have been used in both, discrete [3–11] and continuous magnetic systems [12–15]. Nonlinear time-dependent problems in magnetism have been studied in numerous cases and recent accounts of the state of the art can be found in [16–19]. In particular, phase diagrams of the chaotic regions for magnetic particles

D. Urzagasti
Instituto de Investigaciones Físicas, UMSA, P.O. Box 8635, La Paz, Bolivia

D. Becerra-Alonso
Universidad Loyola Andalucía, 14004 Córdoba, Spain

L.M. Pérez · H.L. Mancini
Departamento de Física y Matemática Aplicada,Universidad de Navarra,
31080 Pamplona, Spain

D. Laroze (✉)
Instituto de Alta de Investigación, Universidad de Tarapacá, Casilla 7D, Arica, Chile
e-mail: dlarozen@uta.cl

D. Laroze
SUPA School of Physics and Astronomy, University of Glasgow, Glasgow G12 8QQ, UK

© Springer International Publishing Switzerland 2016

M. Tlidi and M.G. Clerc (eds.), *Nonlinear Dynamics: Materials, Theory and Experiments*, Springer Proceedings in Physics 173,
DOI 10.1007/978-3-319-24871-4_20

in the presence of time dependent magnetic fields have been given and explored [8–11]. Some of these models show new possible roots and ranges of physical parameters in chaotic domains that could motivate new experiments in this area.

Applications on two-particle systems under constant magnetic fields can be found in [20–23]. For conservative systems, when the interaction between the particles is based on energy exchange, it is possible to obtain analytical expressions for the magnetisations [20]. However, if the anisotropy energy is included, the system becomes non-linear and the analytical solutions are non-tractable. Furthermore, the system can exhibit chaotic states in the conservative case [23]. Two interacting dipoles in the presence of an external homogeneous magnetic field were studied in [24]. The authors found that the total magnetisation is not conserved. The non-dissipative case is a fluctuating function of time with a strong dependence on the strength of the dipolar term. In the dissipative case there is a transient time before the total magnetisation reaches its constant value. However, no permanent chaotic states were found. Recently, we have studied the effect of a time dependent magnetic field on the magnetisation processes of two anisotropic particles [25]. The main dynamical indicators were the Lyapunov exponents [26, 27]. The dynamics of this system was represented in the parameter space, displaying regions with different spatio-temporal behaviour that in this case could be regular or chaotic. Different combinations of parameter values bring the system to solutions that could be periodic, multi-periodic or more complex oscillations with chaotic or hyper-chaotic dynamics (when two or more Lyapunov exponents are positive).

On the other hand, the interaction between the two particles or two coherent dynamical systems can produce different kinds of synchronisation (complete, phase, lag, etc.) [28]. Synchronisation between chaotic systems has been studied in temporal systems and in spatio-temporal systems with symmetries beyond the classical master-slave coupling [29, 30] and it has been widely reviewed in [31–33]. Also, the effects of anisotropies in the coupling have been studied [34]. It is now well known that synchronisation in the presence of anisotropies could enhance synchronisation [35] or suppress chaotic behaviour in 3D systems [36]. In hyper-chaotic systems, synchronisation is achieved without chaos suppression, but the complexity of the system could be modified [37, 38]. Other works regarding synchronism in hyper-chaotic models can be found in [39–43].

The aim of this chapter is to analyse the influence of a time dependent external magnetic field on the synchronisation in a system of two interacting anisotropic magnetic particles. We consider that particles are coupled through a dipole-dipole interaction. The applied external time-dependent field produces a periodic driving in the direction perpendicular to the main anisotropy direction. Phase diagrams indicating different oscillation states, and details about chaotic and hyper-chaotic synchronisation regimes are presented. The manuscript is organised as follows, in Sect. 2, the theoretical model is briefly described. In Sect. 3, the numerical results are provided and discussed. Finally, some conclusions are presented in Sect. 4.

2 Theoretical Model

Let us consider two anisotropic magnetic particles in the presence of an external magnetic field, $\mathbf{H}_{ext}$. We assume that each particle can be represented by a magnetic mono-domain of magnetisation $\mathbf{M}_i$ with $i = (1, 2)$. This approximation is called *macrospin* approximation. The temporal evolution of the system can be modelled by the Landau-Lifshitz equation [1]

$$\frac{d\mathbf{M}_i}{dt} = -|\gamma|\mathbf{M}_i \times \mathbf{H}_i - \frac{\eta|\gamma|}{M_{iS}}\mathbf{M}_i \times (\mathbf{M}_i \times \mathbf{H}_i)\,, \tag{1}$$

where, γ is the gyromagnetic factor, which is associated with the electron spin and is approximately given by $|\gamma| = |\gamma_e|\,\mu_0 \approx 2.21 \times 10^5\,\mathrm{m\,A^{-1}\,s^{-1}}$. In the above equation, η denotes the dimensionless phenomenological damping coefficient that is characteristic of the material and has a typical value ranging from 10^{-4} to 10^{-3} in garnets and 10^{-2} or larger in cobalt or permalloy [44]. We assume that the coupling between the particles is the dipole-dipole interaction, hence the effective magnetic field for each particle, $\mathbf{H}_i$, is given by

$$\mathbf{H}_i = \mathbf{H}_{ext} + \beta_i \left(\mathbf{M}_i \cdot \hat{\mathbf{n}}_i\right)\hat{\mathbf{n}}_i + d^{-3}\left[3(\mathbf{M}_k \cdot \hat{\mathbf{r}})\hat{\mathbf{r}} - \mathbf{M}_k\right], \tag{2}$$

being $(i, k) = 1, 2$ such that $i \neq k$. Here β_i measures the anisotropy along the $\mathbf{n}_i$ axis, d is the fixed distance between the two magnetic moments, and $\hat{\mathbf{r}}$ is a unit vector along the direction between the two particles. Notice that this special type of anisotropy is called uniaxial anisotropy and the constants β_i can be positive or negative depending on the specific substance and sample shape [44] in use. Let us assume that the particles have the same magnitude $M_{s,1} = M_{s,2} = M_s$ and the same anisotropy $\beta_1 = \beta_2 = \beta$ and $\mathbf{n}_1 = \mathbf{n}_2 = \mathbf{n}$. We apply an external magnetic field $\mathbf{H}_{ext}$ that comprises both, a constant longitudinal and a periodic transverse part with a fixed amplitude and frequency

$$\mathbf{H}_{ext} = \mathbf{H}_0 + \mathbf{H}_T \sin(\omega t)\,, \tag{3}$$

where $\mathbf{H}_0$ ($\|\hat{\mathbf{z}}$), $\mathbf{H}_T$ ($\perp\hat{\mathbf{z}}$) and ω are time independent. The axis $\hat{\mathbf{r}}$ is chosen perpendicular to the anisotropy axis, in particular $\hat{\mathbf{r}} = \hat{\mathbf{x}}$. We note that for zero damping, i.e. $\eta = 0$, and without parametric forcing, i.e. $\mathbf{H}_T = \mathbf{0}$, (1) is conservative. Hence, the dissipation and the oscillatory injection of energy move the magnetic particles in and out of the equilibrium. In such a circumstance the magnetisation of the particles may exhibit complex behaviour such as quasi-periodicity, and chaos [3, 7–9, 11].

Finally, let us remark that for each particle, the LL equation has a constant of motion, which is the magnetic modulus $|\mathbf{M}_i|$ [1]. This feature allows the description of the system with two effective variables. Hence, using spherical coordinates, $\mathbf{M}_i = M_{s,i}\,(\cos\phi_i \sin\theta_i, \sin\phi_i \sin\theta_i, \cos\theta_i)^T$, one can find that the canonical variables are $\{\phi_i, \cos\theta_i\} = \{\phi_i, m_{z,i}\}$ [18]. Therefore, these variables will be used for the synchronisation analysis.

3 Simulations

This section is divided in three parts. The first part briefly discusses the quantities used to characterise the different types of synchronisation. The second one, shortly comments the numerical protocols and the equation to be integrated. The last part covers some numerical results and the corresponding analysis.

3.1 Synchronisation and Dynamical Indicators

We study different types of synchronisations measuring the amplitudes $\{m_{z,i}\}$ and the angles $\{\phi_i\}$ with $i = (1, 2)$. The *common-signal based synchronisation* proposed in [29] can be extended to this case, where the interacting dipoles are enough to find different behaviours and degrees of synchronisation. In particular, two measurements are used in the present work to determine synchronisation.

The first one is the Pearson's coefficient. It has been previously used in chaotic systems [35], that in our case can be written as:

$$\rho_z = \frac{\langle (m_{z1} - \langle m_{z1}\rangle)(m_{z2} - \langle m_{z2}\rangle)\rangle}{\sqrt{\langle (m_{z1} - \langle m_{z1}\rangle)^2\rangle}\sqrt{\langle (m_{z2} - \langle m_{z2}\rangle)^2\rangle}}. \tag{4}$$

This coefficient can vary from -1 to 1. These values represent the complete anti-synchronised and synchronised regime, respectively. In the case of $\rho_z = 0$ the system is not synchronised.

In addition, the *phase synchronisation* will be used for interpretation [30, 31]. The similarity function needed in our case is given by:

$$\Delta\Omega = |\Omega_1 - \Omega_2|, \tag{5}$$

where $\Omega_i = \langle \dot{\phi}_i \rangle$ represents the averaged rate of change of ϕ_i. Note that when $\Delta\Omega = 0$, the system has a phase-synchronised state. Also, this is equivalent to $\Omega_1/\Omega_2 = 1$.

On the other hand, in order to characterise the dynamics of (1) the Lyapunov exponents (LEs) are evaluated. This method consists on quantifying the divergence between two initially close trajectories of a vector field [26, 27]. In general, for an effective N-dimensional dynamical system described by a set of equations, $dX^i/d\tau = F^i(\mathbf{X}, \tau)$, the ith-Lyapunov exponent is given by

$$\lambda_i = \lim_{\tau\to\infty}\left(\frac{1}{\tau}\ln\left(\frac{\|\delta X_\tau^i\|}{\|\delta X_0^i\|}\right)\right), \tag{6}$$

where $\|\delta X^i_\xi\|$ is the distance between the trajectories of the ith-component of the vector field at time ξ. They can be ordered by decreasing amplitude: $\lambda_1 \geq \lambda_2 \geq \cdots \geq \lambda_N$. The first two exponents are the largest Lyapunov exponent (LLE) and the second largest Lyapunov exponent (SLLE). Due to the fact that the LLG equation conserves the modulus of each particle $|\mathbf{m}_i|$ and that the applied magnetic field is time dependent, the effective dimension of the phase space is five. From a dynamical system point of view, more than one exponent may become positive for a system of dimension five. Therefore, by exploring the dependence of the LLE on the different parameters of the system, one can identify areas in the control parameter space, where the dynamics is chaotic (LLE positive), and those showing non-chaotic dynamics (LLE vanishing or negative). In addition, when both the LLE and the SLLE have positive values the system is at a *hyper-chaotic* regime. Nevertheless, since this is a one-frequency forced system, at least one of its Lyapunov exponents will always be zero; hence the simplest attractor is a periodic orbit. Another possibility is to have two or three Lyapunov exponents equal to zero. In these cases the system exhibits a two or three-frequency quasi-periodic behaviour. The Lyapunov exponents are presented in the form of 2-D maps as a function of the relevant parameters of the system [27].

The detailed analysis of the parameter space of the Lyapunov exponents for this system was previously presented in a recent work [25]. Hence, here we focus on the synchronised behaviours. We combined both indicators to quantify the synchronised dynamical regimes. For instance, for a fixed set of parameters if $\rho_z \approx -1$ and $\lambda_1 > 0$ the dipoles are in an anti-synchronised chaotic state; or if $\Delta\Omega = 0$ and $\lambda_1 > 0$ the system is in a chaotic phase-synchronised state.

3.2 Numerical Protocols

In order to simplify and speed-up the integration of the equations of motion, dimensionless units are used. This recasts (1) in terms of the magnetisation $\mathbf{m}_i = \mathbf{M}_i/M_s$ and time $\tau = t|\gamma|M_s$ [18]. This normalisation leads to $|\mathbf{m}_i| = 1$. In order to get a better physical insight into the problem, let us evaluate the scales introduced here. Typical values are, e.g. for cobalt materials, $M_s \approx 1.42 \times 10^6$ A/m [18], hence the time scale ($\tau = 1$) is in the picosecond range, $t_s = 1/(|\gamma|M_s) \approx 3.2$ ps. The dimensionless field is $\tilde{\mathbf{h}} = \mathbf{H}/M_s$ with $\tilde{h}_{x,y} \equiv h_{x,y} \sin(\varphi\tau)$, and $\tilde{h}_z \equiv h_z$ where $\varphi = \omega/(|H|M_s)$ is the dimensionless frequency. In order to avoid numerical artefacts [3], it is suitable to solve (1) in the Cartesian representation, namely,

$$\begin{aligned}\frac{dm_{x,i}}{d\tau} =& -(m_{y,i} + \eta\, m_{x,i}m_{z,i})h_z + \left\{(m_{z,i} - \eta\, m_{x,i}m_{y,i})h_y + \eta\,(m^2_{y,i} + m^2_{z,i})h_x\right\}\sin(\varphi\tau)\\ &+ d^{-3}(m_{z,k} + \eta\, m_{y,k}m_{x,i})m_{y,i} - \left\{\beta\, m_{y,i} + d^{-3}(m_{y,k} - \eta\, m_{z,k}m_{x,i})\right\}m_{z,i}\\ &+ 2\eta\, d^{-3}m_{x,k}m^2_{y,i} - \eta\,(\beta\, m_{x,i} - 2d^{-3}m_{x,k})m^2_{z,i}\,,\end{aligned} \tag{7}$$

$$\frac{dm_{y,i}}{d\tau} = (m_{x,i} - \eta\, m_{y,i} m_{z,i}) h_z - \left\{ (m_{z,i} + \eta\, m_{x,i} m_{y,i}) h_x - \eta\, (m_{z,i}^2 + m_{x,i}^2) h_y \right\} \sin(\varphi\tau)$$
$$- \left\{ \beta\, m_{y,i} + d^{-3} m_{y,k} \right\} \eta\, m_{z,i}^2 - d^{-3} (m_{z,k} + 2\eta\, m_{x,k} m_{y,i}) m_{x,i} - \eta\, d^{-3} m_{y,k} m_{x,i}^2$$
$$+ \left\{ \beta\, m_{x,i} - d^{-3} (2 m_{x,k} - \eta\, m_{z,k} m_{y,i}) \right\} m_{z,i}\,, \tag{8}$$

$$\frac{dm_{z,i}}{d\tau} = \left\{ (m_{y,i} - \eta\, m_{x,i} m_{z,i}) h_x - (m_{x,i} + \eta\, m_{y,i} m_{z,i}) h_y \right\} \sin(\varphi\tau)$$
$$+ d^{-3} \left\{ (m_{x,i} m_{y,k} + 2 m_{x,k} m_{y,i}) + \eta\, (m_{y,k} m_{y,i} - 2 m_{x,k} m_{x,i}) m_{z,i} \right\}$$
$$+ \eta\, (m_{x,i}^2 + m_{y,i}^2) \left\{ h_z + \beta\, m_{z,i} - d^{-3} m_{z,k} \right\}\,. \tag{9}$$

Equations (7)–(9) have been integrated by using a fifth order Runge-Kutta integration scheme with a variable step [45] that ensures a relative error of 10^{-7} on the magnetisation fields.

To take the time average in ρ_z and in $\Delta\Omega$ we evolve the system until its initial transient time has been finished and the system is in the persistent state. For both indicators we establish a tolerance lower than 3 % in order to consider the system in a synchronised state. Also, the LEs are calculated for a time span of $\tau = 80{,}000$ after an initial transient time of $\tau = 4000$ has been discarded. The Gram-Schmidt orthogonalisation process is performed after every $\delta\tau = 3.91$. The error has been estimated to be $E = 0.1$ %, which is sufficiently small for the purpose of the present analysis. Due to the large number of parameters involved in the system, $\beta = 1$, $\eta = 0.05$, $h_y = 1$ and $\varphi = 0.5$ will be fixed throughout the calculations. Parameters $\{h_x, h_z, d\}$ will vary depending on the simulation presented.

3.3 Numerical Results

In a system like the one presented in this chapter, synchronised periodic regimes are expected both when the external field or when the dipolar interaction dominates the dynamics. Whenever the external field is strong with respect to the dipolar interaction, dipoles can be expected to be influenced by the field in a synchronised manner. On the other hand, when dipolar interaction dominates, the field can do nothing but slightly perturb the tight orbits of the dipoles, and again, do so in synchronisation. This subsection will however show a broader variety of synchronised states and transitions.

The main results are given in Figs. 1, 2, 3 and 4. In particular, we concentrate the discussion on the influence of the driving field and the distante between particles. Figure 1a shows a color code phase diagram of the Pearson's coefficient ρ_{m_z} as a function of the field amplitudes h_x and h_z. The distance $d = 0.8$ has been chosen for being on the interphase between field prevalence and dipole interaction prevalence. The $h_x \lesssim 1.5$ periodic region shows a very diverse collection of interlaced periodic

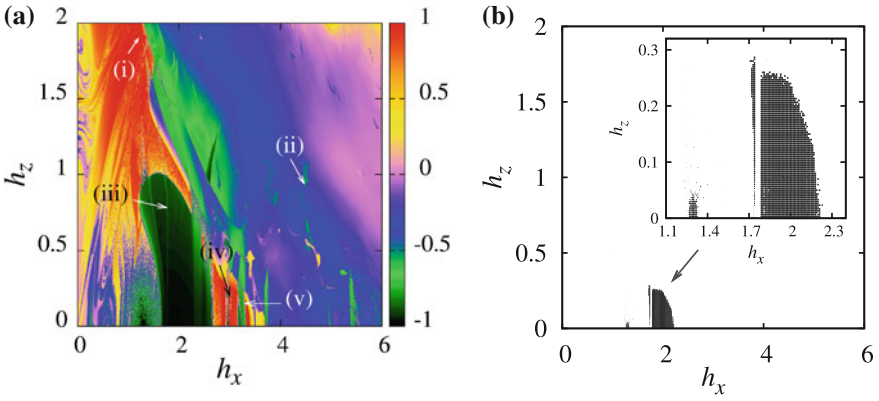


Fig. 1 **a** Phase diagram displaying ρ_z color coded as a function of the field amplitudes h_x and h_z. **b** Region of chaotic anti-synchronisation in frame (**a**) with $|1 + \rho_{m_z}| < 3\,\%$. The fixed parameters are: $\varphi = 0.5$, $\eta = 0.05$, $\beta = 1$, $d = 0.8$ and $h_y = 1$ (Color online)

synchronised and unsynchronised states. Higher h_z in this region mostly have ρ_{m_z} equal to 1 or close to it. Anti-synchronisation occurs in a smaller subregion for $\{0 \lesssim h_z \lesssim 0.2, 1 \lesssim h_x \lesssim 1.5\}$. The chaotic tongue-shaped region within $\{0 \lesssim h_z \lesssim 1, 1.5 \lesssim h_x \lesssim 2.5\}$, is anti-synchronised. This means that entering the tongue from, for instance, lower values of h_x implies a transition from periodic unsynchronised regimes, to chaotic anti-synchronised ones. The detail of anti-synchronised chaos can be seen in Fig. 1b. However, there are values at the top h_z end of the tongue, and at the top h_x end of it where the dipoles go from synchronised periodicity to anti-synchronized chaos. This interesting transition to anti-synchronisation, precisely when the system earns a degree of instability due to chaos, is at this point unintuitive to explain in terms of analysis. The remaining chaotic region with $h_z \gtrsim 0.8(3.5 - h_x)$ is predominantly unsynchronised in terms of the Pearson's coefficient.

Several periodic-state parameters were indicated in Fig. 1a. Their trajectories of the first particle and the corresponding Fourier spectrum of $m_{z,1}$ are detailed in Fig. 2. We note that all trajectories presented have a high number of Fourier peaks. The simplest one is row (i), still found in the $h_z \lesssim 0.8(3.5 - h_x)$ region, where simple dynamics are more common (except for the chaotic tongue). Of the five cases presented, row (ii) has the most Fourier peaks. The figures show an intricate periodic orbit where the two dipoles are in antisymmetry. The other cases are all symmetric periodic orbits where one of the m_x poles prevails over the other, depending on the initial conditions. In addition, we can observe that there are periodic synchronisation in cases (i), (iv) and (v).

The first three frames of Fig. 3 show color code phase diagrams of the Pearson's coefficient as a function of the field amplitude h_x and the distance d. The Pearson's coefficient exhibits a complex topology in the parameters space. Multiple transitions

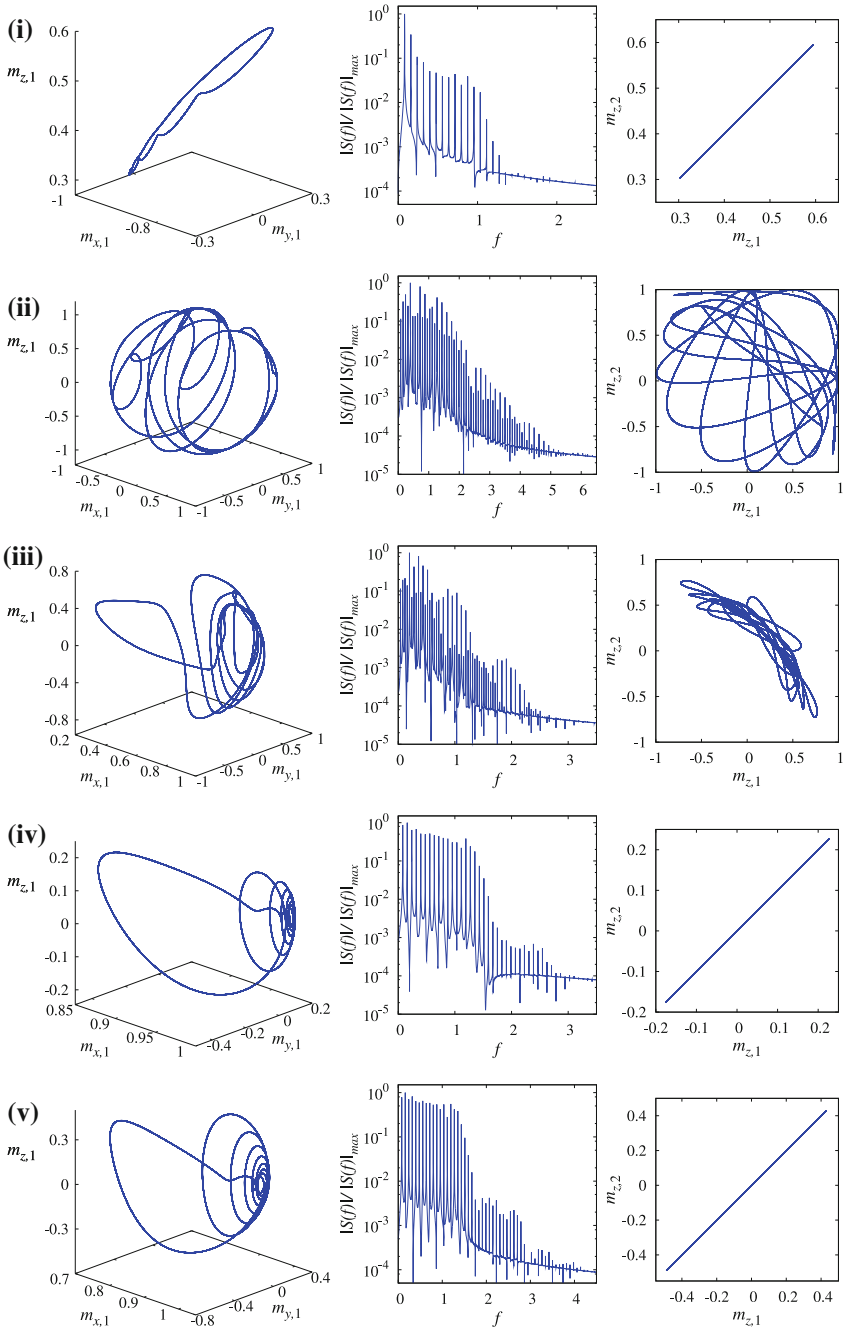


Fig. 2 3D trajectory of $\mathbf{m}_1$ (column 1), normalised FTT of $m_{z,1}$ (column 2) and parametric plot of $(m_{z,1}, m_{z,2})$ (column 3) of the instances indicated in Fig. 1a

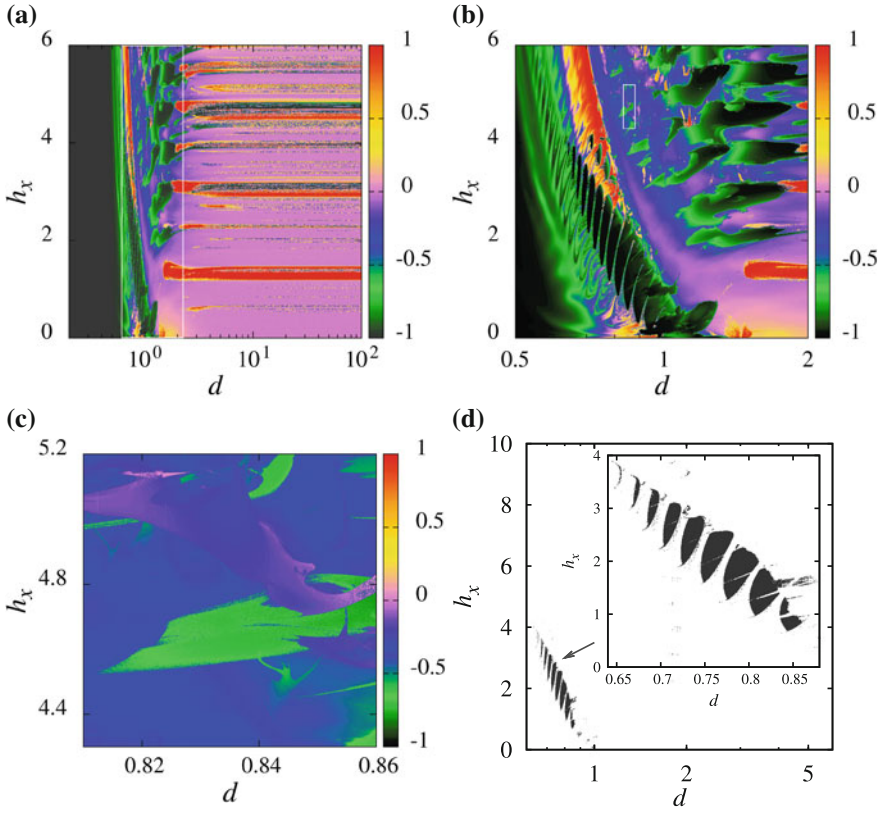


Fig. 3 **a** Phase diagram displaying ρ_{m_z} coded as a function of the field amplitude h_x and the distance d. **b** Magnification of the *white* box in (**a**). **c** Magnification of the white box in (**b**). **d** Zoom on the region (**b**) with chaotic anti-synchronisation with $|1 + \rho_{m_z}| < 3\,\%$. The fixed parameters are: $\varphi = 0.5$, $\eta = 0.05$, $\beta = 1$, $h_y = 1$ and $h_z = 0.1$ (Color online)

between synchronised to non-synchronised regimes can be observed. In fact, it outlines the similar features found in the LLE results of [25]. Frames (b) and (c) are successive magnifications of frame (a) for intermediate values of d. The characteristic shapes within $h_x \lesssim 2.0(1 - d)$ (as seen in frame (b)) are predominantly anti-synchronised, although sparse regimes of synchronised chaos are also found as it is shown in frame (d). The zoom presented in Fig. 3 frame (c) shows a granulated parametric space tending to anti-synchronisation, surrounded by non-synchronised regimes. Hyper-chaotic synchronisation was not found for these set of parameters.

Finally, Fig. 4 shows the phase synchronisation as a function of field amplitude h_x and the distance d. Here we focus on intermediate values of the distance. Phase synchronisation is prevalent for most of the range studied, with the exception of islands past $d \gtrsim 1$ (frames (d) and (e)). There is almost no phase synchronisation

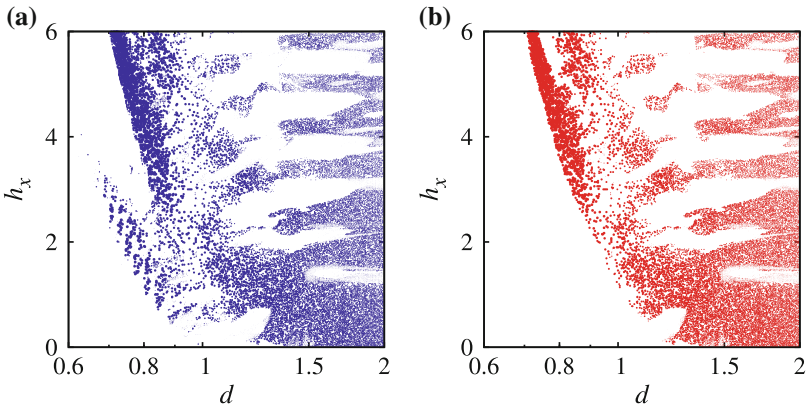


Fig. 4 Region of chaotic (**a**) and hyper-chaotic syncronisation (**b**) as a function of the field amplitude h_x and the distance d with $|1 - \Omega_1/\Omega_2| < 3\,\%$. The fixed parameters are: $\varphi = 0.5$, $\eta = 0.05$, $\beta = 1$, $h_y = 1$ and $h_z = 0.1$ (Color online)

for $1 \lesssim d \lesssim 1.5$ and $0 \lesssim h_x \lesssim 0.1$. We can observe that there are hyper chaotic phase-synchronised states as it shown in frame (b). These regions are subsets of the chaotic ones.

4 Final Remarks

The magnetisation dynamics of two anisotropic magnetic particles interacting via dipolar interaction in the presence of a constant longitudinal external magnetic field and a periodic transversal field has been studied using the dissipative Landau-Lifshitz equation. The system presents a variety of regular and (hyper-)chaotic regimes, such that the regular regions consist on either periodic or quasi-periodic solutions [25]. We have focused on the synchronisation phenomena. The different types of synchronisation have been measured using two main indicators: the Pearson's coefficient associated to the z-components of the magnetic moments and the difference between the phases. The latter is common for most of the parametric regimes presented, which is expectable whenever dipole interaction is predominant. However, the measurement of the Pearson's coefficient has provided with the analysis of four possible states: chaotic synchronisation, hyper-chaotic synchronisation, chaotic anti-synchronisation, and hyper-chaotic anti-synchronisation. The last one has not been found. Regarding the other three states: hyper-chaos is of course a subset of chaos in the parametric space. Synchronised hyper-chaos is never found in the vicinity of anti-synchronised chaos. Chaos-periodicity transitions, in terms of synchronisation, are also diverse. Periodic synchronisation is borderline with chaotic anti-synchronised states, as the field is increased both in the h_x and h_z directions.

Acknowledgments DU acknowledges the PhD fellowship from the Performance Agreement Project UTA/Mineduc (Universidad de Tarapacá). DBA was supported in part by the Spanish Inter-Ministerial Commission of Science and Technology under Project TIN2014-54583-C2-1-R, the European Regional Development fund, and the "Junta de Andalucía" (Spain), under Project P2011-TIC-7508. LMP and HLM acknowledge partial financial support from the Spanish Ministry of Science and Technology under Contract No. FIS2011-24642 and FIS2014-54101. DL acknowledges partial financial support from Basal Program Center for Development of Nanoscience and Nanotechnology (CEDENNA), UTA-project 8750-12 and Engineering and Physical Sciences Research Council Grant No. EP/L002922/1.

References

1. L. Landau, *Collected Papers of Landau* (Pergamon, New York, 1965)
2. T.L. Gilbert, A phenomenological theory of damping in ferromagnetic materials. IEEE Trans. Mag. **40**, 11613 (2004)
3. L.F. Alvarez, O. Pla, O. Chubykalo, Quasiperiodicity, bistability, andchaosinthe Landau-Lifshitz equation. Phys. Rev. B **61**, 11613 (2000)
4. D. Laroze, L.M. Perez, Classical spin dynamics of four interacting magnetic particles on a ring. Phys. B **403**, 473 (2008)
5. P. Diaz, D. Laroze, Configurational temperature for interacting anisotropic magnetic particles. Int. J. Bifurcat. Chaos **19**, 3485 (2009)
6. D.V. Vagin, P. Polyakov, Control of chaotic and deterministic magnetization dynamics regimes by means of sample shape varying. J. Appl. Phys. **105**, 033914 (2009)
7. R.K. Smith, M. Grabowski, R.E. Camley, Period doubling toward chaos in a driven magnetic macrospin. J. Magn. Magn. Mater. **322**, 2127 (2010)
8. J. Bragard, H. Pleiner, O.J. Suarez, P. Vargas, J.A.C. Gallas, D. Laroze, Chaotic dynamics of a magnetic nanoparticle. Phys. Rev. E **84**, 037202 (2011)
9. D. Laroze, J. Bragard, O.J. Suarez, H. Pleiner, Characterization of the chaotic magnetic particle dynamics. IEEE Trans. Mag. **47**, 10 (2011)
10. D. Laroze, D. Becerra-Alonso, J.A.C. Gallas, H. Pleiner, magnetization dynamics under a quasiperiodic magnetic field. IEEE Trans. Magn. **48**, 3567 (2012)
11. L.M. Pérez, J. Bragard, H.L. Mancini, J.A.C. Gallas, A.M. Cabanas, O.J. Suarez, D. Laroze, Netw. Heterog. Media **10**, 209 (2015)
12. A.M. Kosevich, B.A. Ivanov, A.S. Kovalev, Magnetic solitons. Phys. Rep. **194**, 117 (1990)
13. I.V. Barashenkov, M.M. Bogdan, V.I. Korobov, Stability diagram of the phase-locked solitons in the parametrically driven, damped nonlinear Schrödinger equation. Europhys. Lett. **15**, 113 (1991)
14. M.G. Clerc, S. Coulibaly, D. Laroze, Localized states and non-variational Ising-Bloch transition of a parametrically driven easy-plane ferromagnetic wire. Phys. D **239**, 72 (2010)
15. A.O. León, M.G. Clerc, S. Coulibaly, Traveling pulse on a periodic background in parametrically driven systems. Phys. Rev. E. **91**, 050901 (2015)
16. P.E. Wigen (ed.), *Nonlinear Phenomena and Chaos in Magnetic Materials* (World Scientific, Singapore, 1994)
17. B. Guo, S. Ding, *Landau Lifshitz Equations* (World Scientific, Singapore, 2008)
18. I.D. Mayergoyz, G. Bertotti, C. Serpico, *Nonlinear Magnetization Dynamics in Nanosystems* (Elsevier, Dordrech, 2009). and references therein
19. M. Lakshmanan, The fascinating world of the Landau-Lifshitz-Gilbert equation: an overview. Phil. Trans. R. Soc. A **369**, 1280 (2011)
20. D. Mentrup, J. Schnack, M. Luban, Spin dynamics of quantum and classical Heisenberg dimers. Phys. A **272**, 153 (1999)

21. D.V. Efremov, R.A. Klemm, Heisenberg dimer single molecule magnets in a strong magnetic field. Phys. Rev. B **66**, 174427 (2002)
22. D. Laroze, P. Vargas, Dynamical behavior of two interacting magnetic nanoparticles. Phys. B **372**, 332 (2006)
23. L.M. Pérez, O.J. Suarez, D. Laroze, H.L. Mancini, Classical spin dynamics of anisotropic Heisenberg dimers Cent. Eur. J. Phys. **11**, 1629 (2013)
24. D. Laroze, P. Vargas, C. Cortes, G. Gutierrez, Dynamics of two interacting dipoles. J. Magn. Magn. Mater. **320**, 1440 (2008)
25. D. Urzagasti, D. Becerra-Alonso, L.M. Pérez, H.L. Mancini, D. Laroze, *Hyper-chaotic magnetisation dynamics of two interacting dipoles* (Submitted)
26. A. Wolf, J.B. Swift, H.L. Swinney, J.A. Vastano, Determining Lyapunov exponents from a time series. Phys. D **16**, 285 (1985)
27. J.A.C. Gallas, The structure of infinite periodic and chaotic hub cascades in phase diagrams of simple autonomous flows. Int. J. Bifur. Chaos **20**, 197 (2010). and references therein
28. A. Pikovsky, M. Rosenblum, J. Kurths, *Synchronization* (A Universal Concept in Nonlinear Sciences). (Cambridge University Press, Cambridge, 2001)
29. L.M. Pecora, T.L. Carroll, Synchronization in chaotic systems. Phys. Rev. Lett. **64**, 821 (1990)
30. A.S. Pikovsky, M.G. Rosenblum, J. Kurths, Synchronization in a population of globally coupled chaotic oscillators. Europhys. Lett. **34**, 165 (1996)
31. M.G. Rosenblum, A.S. Pikovsky, J. Kurths, From phase to lag synchronization in coupled chaotic oscillators. Phys. Rev. Lett. **78**, 4193 (1997)
32. S. Boccaletti, J. Kurths, G. Osipov, D. Valladares, C. Zhou, The synchronization of chaotic systems. Phys. Rep. **336**, 1 (2002)
33. S. Boccaletti, *The Synchronized Dynamics of Complex Systems* (Elsevier, Dordrech, 2009)
34. J. Bragard, S. Boccaletti, H. Mancini, Asymmetric coupling effects in the synchronization of spatially extended chaotic systems. Phys. Rev. Lett. **91**, 064103 (2003)
35. J. Bragard, S. Boccaletti, C. Mendoza, H.G.E. Hentschel, H. Mancini, Synchronization of spatially extended chaotic systems in the presence of asymmetric coupling. Phys. Rev. E **70**, 036219 (2004)
36. J. Bragard, G. Vidal, H. Mancini, C. Mendoza, S. Boccaletti, Chaos suppression through asymmetric coupling. Chaos **17**, 043107 (2007)
37. G. Vidal, H. Mancini, Hyperchaotic synchronization under square symmetry. Int. J. Bifurcat. Chaos **19**, 719 (2009)
38. G. Vidal, H. Mancini, Hyperchaotic synchronization. Int. J. Bifurcat. Chaos **20**, 885 (2010)
39. Y-C. Lai, Synchronism in symmetric hyperchaotic systems, Phys. Rev. E **55**, R4861 (1997)
40. L. Yaowen, G. Guangming, Z. Hong, W. Yinghai, G. Liang, Synchronization of hyperchaotic harmonics in time-delay systems and its application to secure communication. Phys. Rev. E **62**, 7898 (2000)
41. A.A. Budini, Langevin approach to synchronization of hyperchaotic time-delay dynamics. J. Phys. A: Math. Theor. **41**, 445001 (2008)
42. C. Li, Y. Tong, H. Li, K. Su, Adaptive impulsive synchronization of a class of chaotic and hyperchaotic systems. Phys. Scr. **86**, 055003 (2012)
43. H.-M. Li, C.-L. Li, Switched generalized function projective synchronization of two identical/different hyperchaotic systems with uncertain parameters. Phys. Scr. **86**, 045008 (2012)
44. R.C. O'Handley, *Modern Magnetic Materials: Principles and Applications* (Wiley-Interscience, USA, 1999)
45. W.H. Press, S.A. Teukolsky, W.T. Vetterling, B.P. Flannery, *Numerical Recipes in FORTRAN* (Cambridge University Press, UK, 1992)